Bulgarian Chemical Communications, Volume 56, Issue 3 (pp. 208-214) 2024 DOI: 10.34049/bcc.56.3.EN-M

Modeling of continuous-flow phenol adsorption onto acrylonitrile-divinylbenzene copolymer

E. Neziri, D. Duranoğlu*

Yildiz Technical University, Chemical Engineering Department, 34220, Esenler, İstanbul, Turkey

Received June 3, 2024; Accepted: August 17, 2024

Phenol, a highly toxic organic compound, is commonly found in industrial effluents of pharmaceuticals, paper, plastics, and petrochemicals production processes. Effective treatment techniques should be enhanced to reduce the negative effects of phenol contamination in water sources, which poses serious environmental risks. An efficient option for treating water sources polluted with phenol is the continuous adsorption technique. Due to high mechanical strength, large surface area, ease of regeneration, and cost-effectiveness, polymeric structures are promising adsorbents. In this study, continuous-flow phenol adsorption onto acrylonitrile-divinylbenzene (AN-DVB) copolymer was investigated. Phenol adsorption was modeled in order to characterize the adsorption process, and the predictive accuracy of the models under continuous flow conditions was evaluated. A phenol aqueous solution was passed through a fixed column packed with AN-DVB copolymer beads at room temperature. Longer breakthrough and exhaustion periods were obtained by increasing the amount of adsorbent in the column; however, shorter breakthrough and exhaustion times and lower adsorption capacity were obtained by increasing the flow rate without altering the amount of adsorbent. The experimental breakthrough curves were modeled with Adams & Bohart, Thomas, Yoon & Nelson, Clark and modified dose-response column models *via* non-linear regression analysis. For every condition under investigation, the modified dose-response model provided a good fit with the experimental data. Isopropanol was found to successfully regenerate polymer beads through adsorption-desorption cycles.

Keywords: Adsorption; Modeling; Phenol; Acrylonitrile-divinylbenzene copolymer; Continuous process.

INTRODUCTION

Phenol (C_6H_5OH) is a widely used aromatic compound that can be found in the wastewater of manufacturing processes, such as pharmaceuticals, petroleum refineries. etc. [1, 2]. It is toxic to humans, plants and aquatic organisms at small dosage; therefore, it was classified as a priority pollutant by the United States Environmental Protection Agency. Phenol concentration was limited to 1 μg/L by World Health Organization [1]. Although in order to remove phenol from water resources, different methods such as adsorption, distillation, advanced oxidation processes, etc. have been studied [3], the most favorable is the highly effective low-cost adsorption process [4]. The usage of polymers as adsorbents is promising due to their low cost, easy regeneration, controllable pore structure and high mechanical strength [5].

Since most plants are operated in continuous process, studying under continuous flow is very important for the industrial applications. Studies on phenol removal in a fixed-bed column using activated carbon [6] and polymeric structures [7] have been conducted. Fixed-bed columns have easy industrial application, offering data on the concentration of pollutants in the effluent as a function of time [8].

The aim of this study is to investigate and model the adsorption of phenol onto acrylonitrile-divinylbenzene copolymer (AN-DVB) in a continuous process. Breakthrough curve data obtained at different column bed heights and flow rates were modeled using Adams & Bohart, Thomas, Yoon & Nelson, Clark and modified-dose response models. Regeneration of AN-DVB polymers using isopropanol was also studied.

EXPERIMENTAL

Fixed-bed adsorption studies

A specified amount of AN-DVB was placed in a glass column with glass filter to prevent particle loss. Peristaltic pump was used to constantly feed a 25 mg/L phenol solution to the column at room temperature. Samples were gathered at different time intervals and the phenol concentration was measured using UV spectrophotometry at 270 nm. Conditions for the experiments are given in Table 1.

* To whom all correspondence should be sent:
E-mail: *dilekdur@gmail.com, dduran@yildiz.edu.tr*

Table 1. Experimental conditions of fixed-bed column studies

Exp. no	C_0 (mg/L)	Weight of adsorbent (g)	Q (mL/min)	Bed height (mm)	D (mm)
1	25.0	0.1722	1	13.73	10.4
2	25.0	0.6888	1	42.51	10.4
3	25.0	0.6888	5	42.51	10.4

- *Analysis of column data*

Column data was analyzed using the equations given below [9]. Effluent volume was calculated using Equation (1):

$$V_{eff}\,(mL) = Q \cdot t_{total} \quad (1)$$

where Q is the volumetric flow rate (mL/min) and t_{total} is total flow time (min). The amount of phenol adsorbed throughout the column is notated as q_{total} and it was calculated using Equation (2) where A is the area under the curve of adsorbed phenol concentration ($C_{ad} = C_0–C_t$) against time, and Q is the volumetric flow rate (mL/min).

$$q_{total}(mg) = \frac{Q \cdot A}{1000} \quad (2)$$

Amount of phenol that passed through column was found using Equation (3):

$$m_{total}(mg) = \frac{C_0 \cdot Q \cdot t_{total}}{1000} \quad (3)$$

Unadsorbed phenol concentration at equilibrium C_{eq} (mg/L) was found using Equation (4):

$$C_{eq}(mg/L) = \frac{m_{total} - q_{total}}{V_{eff}\,1000} \quad (4)$$

where V_{eff} is the effluent solution volume in mL. Total phenol removal was calculated by Equation (5):

$$\text{Total removal of phenol (\%)} = \frac{q_{total}}{m_{total}} \cdot \quad (5)$$

The maximum adsorption capacity of the column (q_{eq}) was calculated using Equation (6):

$$q_{eq}(mg/g) = \frac{q_{total}}{X} \quad (6)$$

where X is amount (g) of adsorbent in the column.

Breakthrough capacity was calculated by following the same steps at the breakthrough point.

Effective capacity utilization (%) was calculated using Equation (7):

$$\text{Effective capacity utilization (\%)} = \frac{Breakthrough\ capacity}{\text{Total capacity}} \cdot 100 \quad (7)$$

- *Modeling of fixed-bed adsorption data*

Five different models (Adams & Bohart, Thomas, Yoon & Nelson, Clark and modified dose-response) were employed for modeling experimental data. The parameters of the given models were obtained using a curve fitting toolbox in MATLAB 2022b software.

Adams & Bohart model. This model is based on the theory of surface reaction, indicating that the reaction is not immediate. This model assumes that adsorption is related to flow rate, flow concentration and amount of adsorbent. However, this model is more accurate in the initial part of the breakthrough curve (C_t<0.5 C_0) [10, 11]. It is expressed in Equation (8):

$$\frac{C_t}{C_0} = \frac{1}{e^{(k_{AB} \cdot N_0 \frac{Z}{U} - k_{AB} \cdot C_0 \cdot t)} + 1} \quad (8)$$

where k_{AB} (L/mg min) is the Adam & Bohart model's kinetic constant, N_0(mg/L) is the capacity per volume in fixed bed, Z (mm) is the bed depth of column, U (mm/min) is the linear velocity and C_0 and C_t (mg/L) are the inlet concentration and outlet concentration, respectively.

Thomas model. Thomas model assumes that adsorption is based on a second-order reversible reaction rather than mass transfer, which can be a drawback since interphase mass transfer can have significant control on column adsorption [12]. The Thomas model is expressed in Equation (9):

$$\frac{C_t}{C_0} = \frac{1}{e^{(k_{th} \cdot q_0 \cdot \frac{X}{Q} - k_{Th} \cdot C_0 \cdot t)} + 1} \quad (9)$$

where k_{Th} (mL/min·mg) is Thomas kinetic coefficient, q_0 (mg/g) maximum adsorption capacity, Q (mL/min) volumetric flow rate and X (g) is mass of adsorbent in the column.

Modified dose-response model. Modified dose-response model is a regulation of the Thomas model. It reduces the errors of the Thomas model especially in the lower and higher breakthrough curve times [13]. The modified dose-response model is expressed in Equation (10):

$$\frac{C_t}{C_0} = 1 - \frac{1}{\left(\frac{C_0 \cdot Q \cdot t}{q_0 \cdot X}\right)^a + 1} \quad (10)$$

where *a* is a modified dose-response model's parameter.

Yoon & Nelson model. It is based on the assumption that the probability of adsorption for each sorbate molecule is inversely proportional to the probability of sorbate sorption and sorbate breakthrough on the sorbent [12]. Yoon & Nelson model is shown in Equation (11):

$$\frac{C_t}{C_0} = \frac{1}{e^{k_{YN}\cdot(\tau - t)} + 1} \quad (11)$$

where k_{YN} (min^{-1}) is the Yoon–Nelson rate constant and t (min) is the required time for Ct/C_0=0.5.

Clark model. It was developed on the assumption that mass transfer is present in the entire column and that adsorption occurs according to the Freundlich isotherm [14]. It is expressed in Equation (12).

$$\frac{C_t}{C_0} = \frac{1}{\left(1 + A\cdot e^{\cdot(-r\cdot t)}\right)^{\frac{1}{n-1}}} \quad (12)$$

where *A* and *r* are the Clark model constants and n is the Freundlich constant.

Regeneration

The AN-DVB polymers' reusability was evaluated using adsorption-desorption cycles. The used beads were regenerated using isopropanol in a continuous flow column system once each cycle was finished. The polymers were then reintroduced for the following cycle after being thoroughly cleaned with distilled water.

MATERIALS

Suspension polymerization method was used in the preparation of acrylonitrile-divinylbenzene copolymer (AN-DVB), with hexadecane and toluene (1:9 w/w) as diluents. One-third of the mixture was made up of monomers, and the other two-thirds were made up of inert diluents; the crosslinker level was set as 40%. Full details of the polymerization are given in Duranoğlu *et al.* [15]. Characteristics of AN-DVB are given in Table 2. The porous structure of the polymer was examined by nitrogen adsorption method using the Quantachrome Autosorb-1-C surface characterization device. The surface area was calculated using the BET (Brunauer, Emet and Teller) method, and the pore volumes were calculated using the DFT (Density Functional Theory) method and nitrogen adsorption isotherms. These calculations were performed automatically using the Autosorb1 software program. Carbon, nitrogen and hydrogen contents were determined by VarioEL III CHNS elemental analyzer.

Nitrogen adsorption-desorption isotherm of AN-DVB is given in Figure 1A. Nitrogen adsorption of AN-DVB copolymer fits type II isotherm according to IUPAC classification, indicating non-porous or macroporous adsorbent. As seen in Table 2, the micropore volume is very low compared to the total pore volume. In addition, AN-DVB contains mostly acidic functional groups. The relatively low porous structure of AN-DVB copolymer beads can be seen on the SEM images given in Figures 1B and 1C.

Table 2. Characteristics of AN-DVB

Properties	AN-DVB	Ref.
Product yield (%)	82	
BET surface area (m^2/g)	70	[15]
Pore volume (cm^3/g)	0.1430	[15]
Micropore volume (cm^3/g)	0.0260	[15]
Acidic groups (meq/g)[1]	0.5499	
Basic groups (meq/g)[1]	-	

[1]Measured by Boehm method [16]

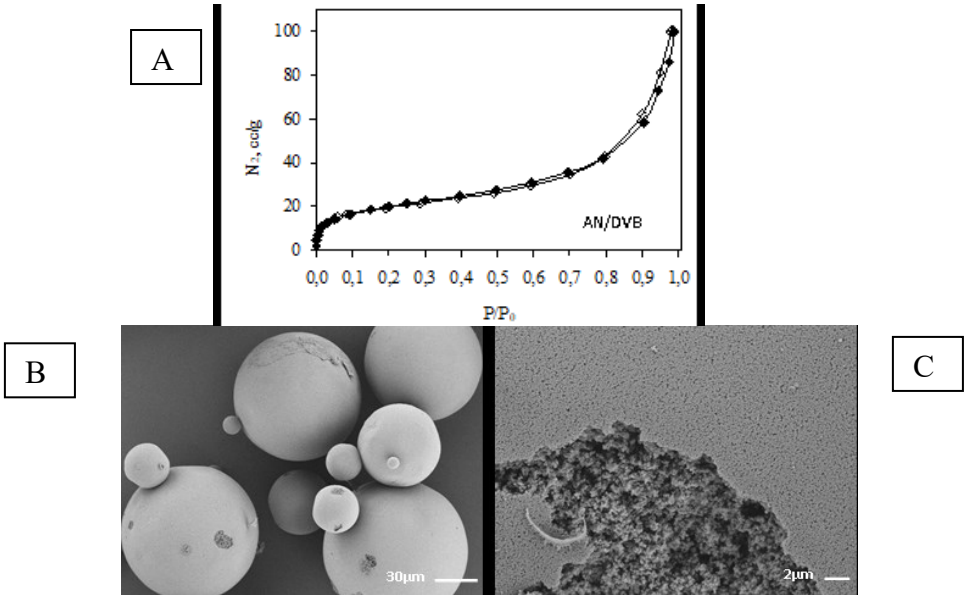

Figure 1. A: Nitrogen adsorption-desorption isotherm (♦: adsorption; ◊: desorption); B, C: SEM images

RESULTS AND DISCUSSION

Results of fixed-bed column studies

Breakthrough curves for each experiment are given in Figure 2. C_t/C_0 increased rapidly and linearly and reached the exhaustion point at around 0.82. After exhaustion point, where the adsorbent capacity reached the maximum, C_t/C_0 showed a slower increase. C_t/C_0 data were also plotted against the bed volume (Figure 3), which was calculated using Equation 13:

$$\text{Bed volume} = \frac{V}{\pi \cdot \frac{D^2}{4} h} \quad (13)$$

where V is effluent solution volume (mL), D is diameter of column (cm), and h is the height of polymer bed (cm).

The column data analysis results are given in Table 3. The effect of bed height was observed by increasing the amount of AN-DVB from Exp. 1 to Exp. 2. Comparing the breakthrough curves (Figure 3) it can be seen that increasing adsorbent amount increased breakthrough and exhaustion times. The amount of adsorbed phenol (q_{total}), as well as total removal % increased with increase in bed height (Table 3). The effect of flow rate was observed without changing the bed height from Exp. 2 to Exp. 3. Increasing flow rate resulted in decreased breakthrough and exhaustion time and lower adsorption capacity and total removal (Table 3). The breakthrough capacities were calculated for the threshold breakthrough point of 0.20. Effective capacity utilization was calculated (Table 4). Despite having a shorter residence time and lower total capacity, Exp. 1 showed a higher breakthrough capacity and effective capacity utilization.

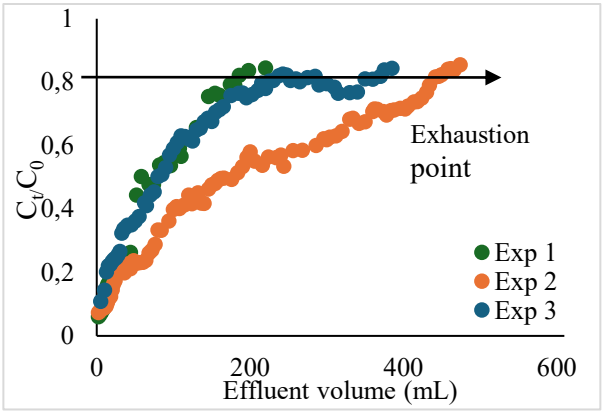

Figure 2. Breakthrough curves for Exps. 1, 2 and 3

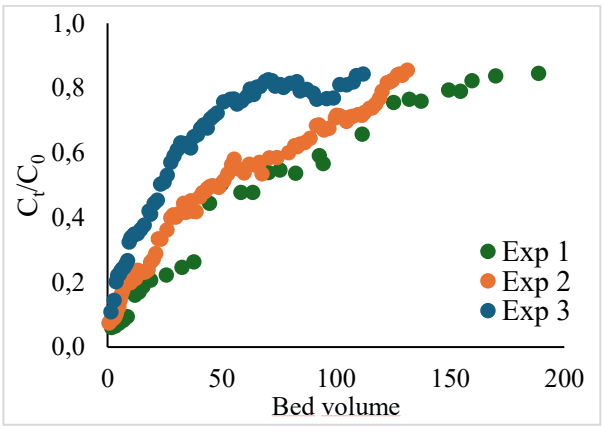

Figure 3. Breakthrough curves with respect to bed volume

Table 3. Results of column data analysis

Exp. no	Bed height (mm)	Adsorbent mass (g)	Q (mL/min)	V_{eff} (mL)	q_{total} (mg)	q_{eq} (mg/g)	Total removal (%)
1	13.73	0.1722	1	186	2.30	13.37	48.74
2	42.51	0.6888	1	442	6.09	8.84	56.69
3	42.51	0.6888	5	238	2.48	3.60	42.97

Table 4. Breakthrough and total capacities

Exp. no	Flow rate Q (mL/min)	Residence time[a] (min)	Breakthrough capacity (mg/g)	Total capacity (mg/g)	Effective capacity utilization (%)
1	1	1.17	2.85	13.37	21.33
2	1	3.61	0.87	8.84	9.84
3	5	0.72	0.39	3.60	10.91

[a] Residence time = Bed volume/Flow rate

Fixed-bed adsorption modeling

The obtained Adams & Bohart model constants are given in Table 5. Adams & Bohart rate constant (k_{AB}) decreased with the increase in bed height (Exp. 1 to Exp. 2) and increased with increase of flow rate (Exp. 2 to Exp. 3.) while the saturation concentration (N_0) decreased with increase of both bed height and flow rate. Correlation coefficient (R^2) values show a relatively good fit between the model and the experimental data.

The maximum adsorption capacity, q_0, and the rate constant, k_{th}, were calculated for Thomas model. The q_0 values decreased with the increase of flowrate and increase of bed height. The theoretical q_0 values are very close to the experimental values. Relatively high R^2 values indicate good fitness between the model and the experimental data, however, they are lower compared to the R^2 values of modified dose-response and Clark models. Modified dose-response model parameters were also estimated and given in Table 5. The found q_0 values were not as close as the Thomas model calculated values. However, modified dose-response model was successful in explaining the breakthrough curve as it can be observed in Figure 4, resulting in higher R^2 values. Compared to other models, obtained R^2 values for each experiment were higher, making it the best fitting model. It can be concluded that the modified dose-response model is the most appropriate model to represent phenol continuous adsorption onto AN-DVB.

Table 5. Fixed-bed adsorption models' parameters

	Exp. 1	Exp. 2	Exp. 3
Adams & Bohart model			
k_{AB} (L/mg·min)	7.60E-04	2.73E-04	0.0021
N_0 (mg/L)	1958.60	1430.70	687.395
R^2	0.944	0.938	0.889
Thomas model			
k_{th} (mL/min·mg)	0.76	0.2725	2.1479
$q_{0,theo}$ (mg/g)	13.26	7.50	3.43
$q_{0,\,exp}$ (mg/g)	13.37	8.84	3.60
R^2	0.944	0.938	0.889
Modified dose-response model			
a	1.286	1.0294	1.036
$q_{0,\,theo}$ (mg/g)	10.442	5.629	2.550
$q_{0,\,exp}$ (mg/g	13.372	8.839	3.600
R^2	0.976	0.973	0.979
Yoon & Nelson model			
k_{YN} (min^{-1})	0.019	0.007	0.052
$t_{\%50,\,theo}$ (min)	89.87	212.65	19.47
$t_{\%50,\,exp}$ (min)	76.91	86.49	16.00
R^2	0.944	0.938	0.889
Clark model			
A	0.062	0.051	0.042
r (min^{-1})	0.014	0.005	0.041
R^2	0.969	0.961	0.922

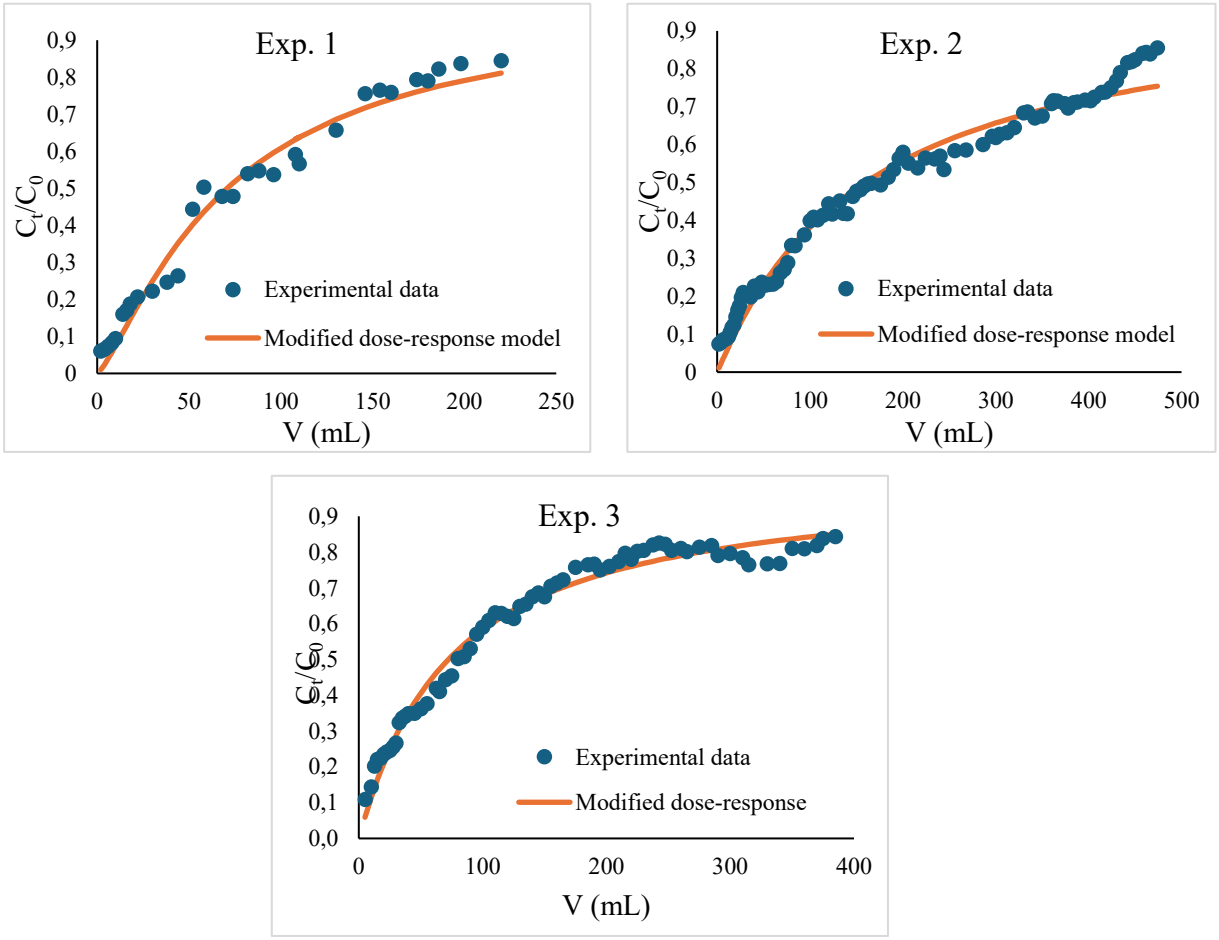

Figure 4. Breakthrough curves of the modified dose-response model

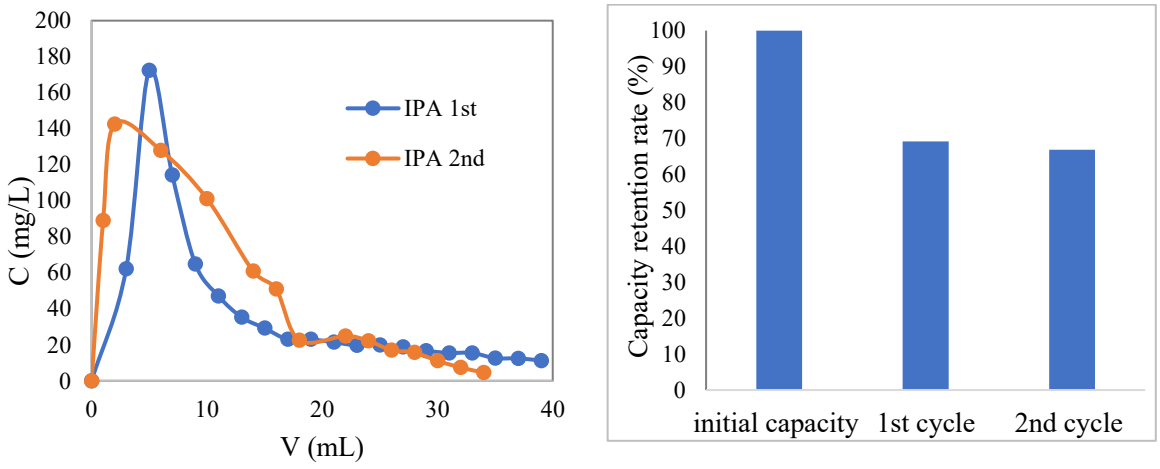

Figure 5. A: Regeneration of AN-DVB beads; B: Adsorption capacity retention rate

Yoon-Nelson model's constants are given in Table 5, where k_{YN} decreased with increase in the bed height and increased with the increase in the flowrate. Although relatively high R^2 values were obtained like in Thomas and Adams & Bohart models, we cannot describe the adsorption process with Yoon-Nelson model due to the fact that the $t_{50\%}$ values are not close to the experimental values. Clark model constants were obtained using the Freundlich constant obtained in batch studies. The Clark model constant A and r decreased as the bed height increased. The R^2 values obtained were higher than for the other models except for the modified dose-response model. As indicated, with Clark model mass transfer plays an important role in the continuous adsorption process. It can be concluded that Clark model can describe the phenol adsorption kinetics on polymer beads in a fixed-bed column.

Regeneration of the polymer beads

Isopropanol (IPA) was found to be effective in desorption of phenol (Figure 5A) in a very short time. Although there is a drop on the adsorption capacity after regeneration, the regenerated polymers maintained the adsorption capacities after the first cycle (Figure 5B). This suggests that IPA is effective in desorbing phenol from the polymer beads while also maintaining the adsorbent's performance.

CONCLUSION

Phenol adsorption onto AN-DVB in a fixed-bed column was studied. Increasing bed height resulted in an increase of the breakthrough and exhaustion times, while increasing the flow rate resulted in a decrease of breakthrough and exhaustion times along with a reduced adsorption capacity. The experimental breakthrough curves fitted very well the modified dose-response model. As the modified dose-response model indicates heterogeneous surfaces and variable adsorption energies, it can be concluded that different interactions with different energy levels like hydrogen bonding, dipole-dipole interactions, and π-π stacking interactions could be responsible for phenol adsorption onto AN-DVB. On the other hand, Clark model was good in describing the kinetics of the adsorption while Thomas model - in estimation of the maximum adsorption capacity. Due to the Thomas model's simplicity and ease of use, it can be used for preliminary designing and scale-up purposes for industrial applications. Clark model kinetic parameters can also be used to determine the size of the adsorption column and the operating conditions. Isopropanol was found to successfully regenerate polymer beads through adsorption-desorption cycles.

REFERENCES

1. Y. Dehmani, D. Dridi, T. Lamhasni, S. Abouarnadasse, R. Chtourou, E. C. Lima, *J. Water Process. Eng.*, **49**, 102965 (2022).
2. K. A. Mohamad Said, A. F. Ismail, Z. Abdul Karim, M. S. Abdullah, A. Hafeez, *Process. Saf. Environ. Prot.*, **151**, 257 (2021).
3. L. G. C. Villegas, N. Mashhadi, M. Chen, D. Mukherjee, K. E. Taylor, N. Biswas, *Curr. Pollu. Rep.*, **2 (**3),157 (2016).
4. J. Zhang, N. Liu, H. Gong, Q. Chen, and H. Liu, *Microporous Mesoporous Mater.*, **336**, 111836 (2022).
5. G. Che-Galicia, J. F. Guayaquil-Sosa, T. Larios-Pachuca, J. A. Galicia-Aguilar, *J. Environ. Chem. Eng.*, **10** (5), 108357 (2022).
6. H. W. Lee, K. J. Kim, A. G. Fane, *Sep. Sci. Technol.*, **32** (11), 1835 (1997).
7. A. Hao, Z. Fu, J. Huang, *Sep. Purif. Technol.*, **311,** 123380 (2023).
8. T. Taweekarn, W. Wongniramaikul, W. Sriprom, W. Limsakul, A. Choodum, *Polym.*, **15,** (19), 3989 (2023).
9. A. P. Lim A. Z. Aris, *Biochem. Eng. J.*, **87**, 50 (2014).
10. R. Han *et al.*, *Chem. Eng. J.*, **149 (**1–3), 123 (2009).
11. J. Goel, K. Kadirvelu, C. Rajagopal, V. K. Garg, *J. Hazard Mater.*, **125** (1-3), 211 (Oct. 2005).
12. Z. Aksu F. Gönen, *Process. Biochem.*, **39 (**5), 599 (2004).
13. G. Yan, T. Viraraghavan, M. Chen, *Adsorpt. Sci. Technol.*, **19 (**1), 25 (2001).
14. R. M. Clark, *Environ. Sci. Technol.*, **21 (**1), 573 (1987).
15. D. Duranoğlu, A. W. Trochimczuk, Ü. Beker, *Chem. Eng. J.*, **165 (**1), 56 (2010).
16. H. P. Boehm, *Carbon,* **40** (1), 145 (2002).